

## **DNS Study on Mechanism of Flow Chaos in Late Boundary Layer Transition**

Yong Yang, Jie Tang, Yonghua Yan, Chaoqun Liu  
University of Texas at Arlington, Arlington, Texas, USA  
Email : cliu@uta.edu

**Abstract.** The mechanism of chaos in late boundary layer transition is a key issue of the laminar-turbulent transition process. A careful study on the characteristic of chaos is carried out by high order direct numerical simulation (DNS). The process of flow chaos was originally considered as a result of large background noise and non-periodic spanwise boundary conditions. However, according to our DNS observation, the loss of symmetry starts from the middle level vortex rings while the top and bottom rings are still symmetric. The non-symmetric structure of second level vortex rings will influence the small scale vortices at the boundary layer bottom quickly. The loss of symmetry at the bottom of the boundary layer quickly spreads to upper level through ejections. This will lead to chaos of the whole flow field. Therefore, the internal instability of multiple level vortex ring structures, especially the middle ring cycles, is the main reason for the process of flow chaos, but not the large background noise. A new numerical simulation and theoretical analysis is carried out on the multiple level vortex ring package stability. The top package is found stable since it is laid out near the inviscid area and the bottom package is found stable since it is constrained by the solid surface. The middle vortex ring package is found most unstable since there is no constraints to the package. The current analysis is focused on the stability of two rotation cores overlapping, which are moving closer and closer. It is found that the flow becomes more unstable when the two cores are moving closer and closer.

## **Nomenclature**

$M_\infty$ = Mach number	$Re$ = Reynolds number
$\delta_{in}$ = inflow displacement thickness	$T_w$ = wall temperature
$T_\infty$ = free stream temperature	$Lz_{in}$ = height at inflow boundary
$Lz_{out}$ = height at outflow boundary	
$Lx$ = length of computational domain along x direction	
$Ly$ = length of computational domain along y direction	



$x_{in}$  = distance between leading edge of flat plate and upstream boundary of computational domain

$\mu_{\infty}$  = viscosity

## 1. Introduction

Turbulence is still covered by a mystical veil in nature after over a century of intensive study. Following comments are made by Wikipedia web page at <http://en.wikipedia.org/wiki/Turbulence>: Nobel Laureate Richard Feynman described turbulence as “the most important unsolved problem of classical physics” (USA Today 2006). According to an apocryphal story, Werner Heisenberg was asked what he would ask God, given the opportunity. His reply was: “When I meet God, I am going to ask him two questions: Why relativity? And why turbulence? I really believe he will have an answer for the first.” (Marshak, 2005). Horace Lamb was quoted as saying in a speech to the British Association for the Advancement of Science, “I am an old man now, and when I die and go to heaven there are two matters on which I hope for enlightenment. One is quantum electrodynamics, and the other is the turbulent motion of fluids. And about the former I am rather optimistic” (Mullin 1989; Davidson 2004).

These comments clearly show that the mechanism of turbulence formation and sustenance is still a mystery for research. Note that both Heisenberg and Lamb were not optimistic for the turbulence study.

The transition process from laminar to turbulent flow in boundary layers is a basic scientific problem in modern fluid mechanics. In order to get deep understanding of the mechanism of the late flow transition in a boundary layer and physics of turbulence, we recently conducted a high order direct numerical simulation (DNS) **with 1920×128×241 grid points and about 600,000 time steps** to study the mechanism of the late stages of flow transition in a boundary layer at a free stream Mach number 0.55 (Chen et al., 2009, 2010a, 2010b, 2011a, 2011b; Liu et al., 1995, 1996, 1997, 2010a, 2010b, 2010c, 2011a, 2011b, 2011c, 2013; Lu et al., 2011, 2011a, 2011b, 2011c, 2012). The work was supported by AFOSR, UTA, TACC and NSF Teragrid. A number of new observations are made and new mechanisms are revealed in late boundary layer transition.

Chaos is a key issue of late boundary layer transition and turbulence formation. This work is devoted to the investigation of the late stages of the laminar-turbulent transition process in a flat-plate boundary layer. As well known, in order to get a fully developed turbulent flow, the following two characteristics should be obtained: 1) small scale vortices; 2) chaos. There are not many existing literatures investigating the mechanism of chaos. Here, we only take those conclusions into account, which were made by Meyer and his co-workers (see Meyer et al 2003). They believe that “the inclined high-shear layer between the legs of the  $\Lambda$ -vortex exhibits increasing phase jitter (i.e chaos) starting from its tip towards the wall region.” However, by carefully

checking our DNS data, we observed a phenomenon which is different from the hypothesis given by Meyer and his co-workers.

A  $\lambda_2$  technology developed by Jeong and Hussain (1995) is used for visualization.

## 2. Case Setup and Code Validation

### 2.1 Case setup

The computational domain is displayed in Figure 1. The grid level is  $1920 \times 128 \times 241$ , representing the number of grids in streamwise ( $x$ ), spanwise ( $y$ ), and wall normal ( $z$ ) directions. The grid is stretched in the normal direction and uniform in the streamwise and spanwise directions. The length of the first grid interval in the normal direction at the entrance is found to be 0.43 in wall units ( $Z^+ = 0.43$ ). The parallel computation is accomplished through the Message Passing Interface (MPI) together with domain decomposition in the streamwise direction (Figure 2). The flow parameters, including Mach number, Reynolds number, etc are listed in Table 1. Here,  $x_{in}$  represents the distance between leading edge and inlet,  $Lx$ ;  $Ly$ ;  $Lz_{in}$  are the lengths of the computational domain in  $x$ -,  $y$ -, and  $z$ -directions, respectively, and  $T_w$  is the wall temperature.

Table 1: Flow parameters

$M_\infty$	$Re$	$x_{in}$	$Lx$	$Ly$	$Lz_{in}$	$T_w$	$T_\infty$
0.5	100	300.79	798.03	22	40	273.15	273.15
	0	$\delta_{in}$	$\delta_{in}$	$\delta_{in}$	$\delta_{in}$	K	K

### 2.2 Code Validation

The DNS code – “DNSUTA” has been validated by NASA Langley and UTA researchers (Jiang et al, 2003; Liu et al, 2010; Lu et al 2011) carefully to make sure the DNS results are correct and reliable. For verification purpose, we only show the skin-friction coefficient and velocity profiles in turbulent wall flow with coarse and fine grids. Detailed comparisons between DNS results with linear theory, experimental and other DNS results can be found from our previous publications.

The skin friction coefficient calculated from the time-averaged and spanwise-averaged profile on a coarse and fine grid is displayed in Figure 5. The spatial evolution of skin friction coefficients of laminar flow is also plotted out for comparison. It is observed from these figures that the sharp growth of the skin-friction coefficient occurs after  $x \approx 450\delta_{in}$ , which is defined as the “onset point”. The skin friction coefficient after transition is in good agreement with

the flat-plate theory of turbulent boundary layer by Ducros, 1996 . Figures 3(a) and 3(b) also show that we get grid convergence in skin friction coefficients.

Time-averaged and spanwise-averaged streamwise velocity profiles for various streamwise locations in two different grid levels are shown in Figure 4. The inflow velocity profiles at  $x = 300.79\delta_{in}$  is a typical laminar flow velocity profile. At  $x = 632.33\delta_{in}$ , the mean velocity profile approaches to a turbulent flow velocity profile (Log law). This comparison shows that the velocity profile from the DNS results is turbulent flow velocity profile and the grid convergence has been realized.

### 3. Our DNS Observations and Analysis on Chaos

#### 3.1 Derivation of Linear Stability Equation

$$\begin{cases} \frac{\partial V}{\partial t} + V \cdot \nabla V = -\nabla p + \frac{1}{Re} \nabla^2 V \\ \nabla \cdot V = 0 \end{cases} \quad (1)$$

Equation (1) denotes the incompressible and non-dimensional Navier-Stokes equations in which,  $V = (u, v, w)$  is the velocity vector. Considering that

$$q(x, y, z, t) = q_0(y) + q'(x, y, z, t) \quad (2)$$

where  $q$  can be specified as  $(u, v, w, p)$ , and  $q_0 = (u_0, v_0, w_0, p_0)$  which represents the value of mean flow, and  $q'$  denotes the corresponding linear perturbation. By eliminating the second order perturbation terms, the linearized governing equation for small perturbations can be written as,

$$\begin{cases} \frac{\partial V'}{\partial t} + (V_0 \cdot \nabla)V' + (V' \cdot \nabla)V_0 + \nabla p' = \frac{\nabla^2 V'}{Re} \\ \nabla \cdot V' = 0 \end{cases} \quad (3)$$

As a first step, a localized 2-D incompressible temporal stability for shear layer is studied. Actually, it relates to the distance among two neighboring vortices in the central streamwise plane. Assume the normal mode is

$$\begin{aligned} V' &= \hat{V}(y) e^{i(\alpha x + \beta z - \omega t)} + c.c. = \hat{V}(y) e^{i\alpha(x + \frac{\beta}{\alpha}z - ct)} + c.c. \\ p' &= \frac{\hat{p}}{\omega} e^{i(\alpha x + \beta z - \omega t)} + c.c. = \hat{p}(y) e^{i\alpha(x + \frac{\beta}{\alpha}z - ct)} + c.c. \\ c &= \frac{\omega}{\alpha} \end{aligned} \quad (4)$$

where  $\hat{V} = (\hat{u}, \hat{v}, \hat{w})$ . The parameter  $\alpha$  is given, which is real and set according to the averaged distance between the new generated rings, and  $c$  should be a complex number. Plugging Equation (4) in Equation (3) yields

$$\begin{aligned}
 L\hat{u} &= Re(Du_0)\hat{v} + i\alpha Re\hat{p} \\
 L\hat{v} &= Re(D\hat{p}) \\
 L\hat{w} &= i\beta Re\hat{p} \\
 i(\alpha\hat{u} + \beta\hat{w}) + D\hat{v} &= 0
 \end{aligned} \tag{5}$$

where  $L = [D^2 - (\alpha^2 + \beta^2) - iRe(\alpha u_0 - \omega)]$ , and  $D = \frac{d}{dy}$ .

Considering in 2D case (without  $w$ ), and by eliminating  $\hat{u}, \hat{p}$ , we can obtain the standard O-S equation on  $\hat{v}$ ,

$$(D^2 - \alpha^2)^2 \hat{v} - i\alpha Re[(U - c)(D^2 - \alpha^2) - D^2 U] \hat{v} = 0 \tag{6}$$

where  $U = u_0$ .

Equation (6) is about  $\hat{v}$ , but we need to get the value of  $c$ . The value of  $c$  determines the property of stability of the equation. Let  $c = c_r + ic_i$ , if  $c_i > 0$ , then the disturbance will continuously grow and the flow would be instable. While if  $c_r$  is greater, the disturbance will grow faster and the flow would be more unstable. But if  $c_i < 0$ , the flow would be stable.

### 3.2 Chebyshev Spectral Method for Linear Stability Analysis

Spectral methods have a significant impact on the accurate discretization of both initial value problems and eigenvalue problems. And spectral method with Chebyshev polynomials has been advantageous, especially in stability analysis of fluid mechanics.

In this stability analysis, the function  $\hat{v}$  could be approximated by Chebyshev expansion,

$$\hat{v}(y) = \sum_{n=0}^{\infty} a_n T_n(y) \approx \sum_{n=0}^N a_n T_n(y) \tag{7}$$

where  $N$  is the number of Chebyshev polynomials used to approximate the velocity profile,  $T_n$  are the Chebyshev polynomials and  $a_n$  are the coefficients. After some algebraic work, Equation (6) yields

$$\left(-U\alpha^2 - U'' - \frac{\alpha^3}{iRe}\right)\hat{v} + \left(U + \frac{2\alpha}{iRe}\right)\hat{v}'' - \frac{1}{i\alpha Re}\hat{v}'''' = c(\hat{v}'' - \alpha^2\hat{v}) \tag{8}$$

By approximating  $\hat{v}$  with a certain Chebyshev expansion, Equation (8) gives

$$\begin{aligned}
 \sum_{n=0}^N \left[ \left(-U\alpha^2 - U'' - \frac{\alpha^3}{iRe}\right) T_n + \left(U + \frac{2\alpha}{iRe}\right) T_n'' - \frac{1}{i\alpha Re} T_n'''' \right] a_n \\
 = c \sum_{n=0}^N a_n (T_n'' - \alpha^2 T_n)
 \end{aligned} \tag{9}$$

If there is no disturbance at the boundary and it will be free stream outside the domain  $(a, b)$ , then we have the corresponding boundary condition for function  $\hat{v}$  as  $\hat{v}(a) = \hat{v}(b) = 0$  and  $D\hat{v}(a) = D\hat{v}(b) = 0$ .

Applying Equation (9) on the whole grids with boundary conditions above, a matrix form of generalized eigenvalue problem is given by

$$A\mathbf{a}^{(\hat{v})} = cB\mathbf{a}^{(\hat{v})} \quad (10)$$

where both  $A$  and  $B$  are the coefficients' matrix and the vector  $\mathbf{a}^{(\hat{v})}$  denotes the vector of  $\{a_n\}$ .  $c$  becomes unknown in the generalized eigenvalue of Equation (10).

### 3.3 Stability Analysis to the Three Velocity Profiles

By solving the general eigenvalue problem for the standard Orr-Sommerfeld equation -- Equation (9) and (10), at  $Re = 1000$  which follows the configuration in the DNS case, the physical solution of the eigenvalue  $c$  is obtained. It shows that these three cases are all unstable. Tab.2 gives the value of generalized eigenvalue  $c$  in three cases (Figures 6-8) and Fig 9 gives the corresponding profile of eigenvector functions.

case	Distance between two rotation centers	Imaginary part of c
1	2.0	0.71482
2	3.0	0.26741
3	4.0	0.20694

Table 2 Results of  $c_i$  for the velocity profile in three cases at  $Re=1000$ ,  $\alpha = 1.0$

By comparison, we can find the image part of  $c$  is the greatest in Case 1 and is the least in Case 3. That means the disturbance will grow faster in Case 1 and slower in Case 3. Note that the distance between two rotation centers is growing from Case 1 to Case 3, and it is reasonable that the disturbance will grow faster and the flow would be more unstable if two rotation centers are closer to each other.

### 4. Some conclusions and future work

The distribution of averaged streamwise velocity are given in Fig 5 along the normal grid lines at the center plane of a ring-like vortex, whose streamwise position is at  $x = 491.1 \delta_{in}$ . The approximations of the base velocity profiles are given in three cases, see Figs 6-8. The distance between two rotation centers are increased from Case 1 to Case 3.

First, our observation is quite different from Meyer et al (2003.) The phenomenon of asymmetry is first observed at the middle level of the overlapping multiple vortex ring cycles instead of the ring tip. The loss of flow symmetry is also found at the middle part of the flow field in the streamwise

direction. The bottom level then loses the symmetry due to the sweeps. Finally, the top flow structure loses the symmetry and the whole flow field becomes chaotic.

The mechanism of chaos in late boundary layer transition is a key issue of the laminar-turbulent transition process. The internal instability of multiple level vortex ring structures, especially the middle ring cycles, is the main reason to cause the asymmetry and then flow chaos, but not the large background noise according to the observation of our DNS computation. A new numerical simulation and theoretical analysis is carried out on the multiple level vortex ring package stability. A two level rotation core overlapping is studied and it is found that the flow becomes more unstable when the two cores are moving closer and closer.

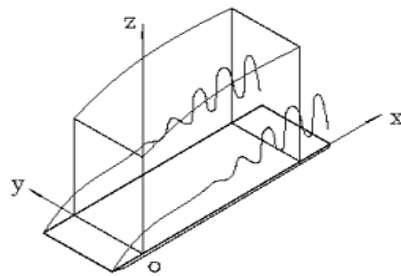


Figure 1: Computation domain

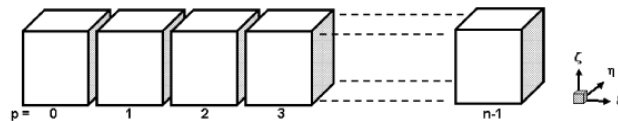
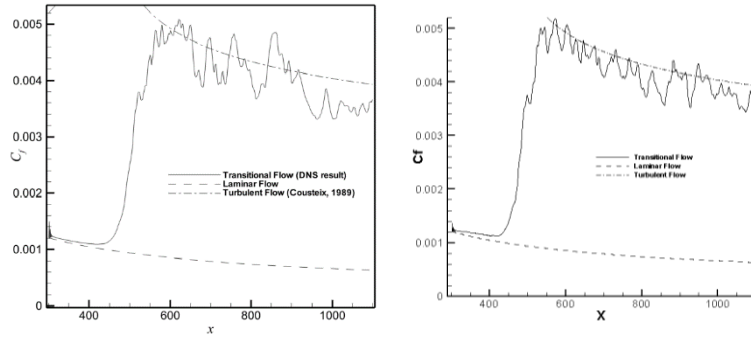
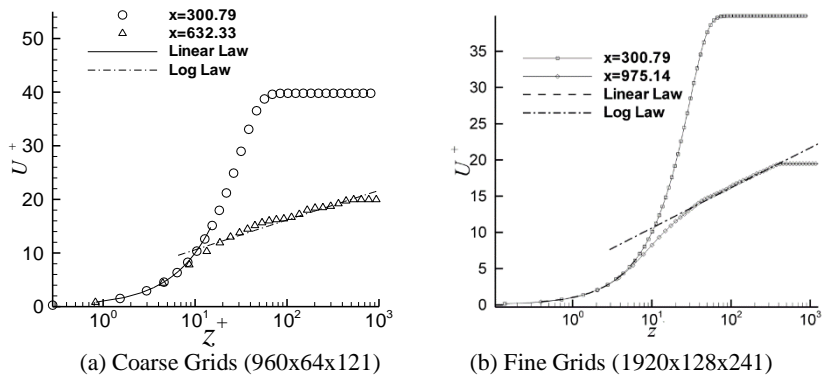


Figure 2: Domain decomposition along the streamwise direction

Also show that we get grid convergence in skin friction coefficients.



(a) Coarse Grids ( $960 \times 64 \times 121$ ) (b) Fine Grids ( $1920 \times 128 \times 241$ )  
 Figure 3: Streamwise evolutions of the time- and spanwise-averaged skin-friction coefficient



(a) Coarse Grids ( $960 \times 64 \times 121$ ) (b) Fine Grids ( $1920 \times 128 \times 241$ )  
 Figure 4: Log-linear plots of the time- and spanwise-averaged velocity profile in wall unit

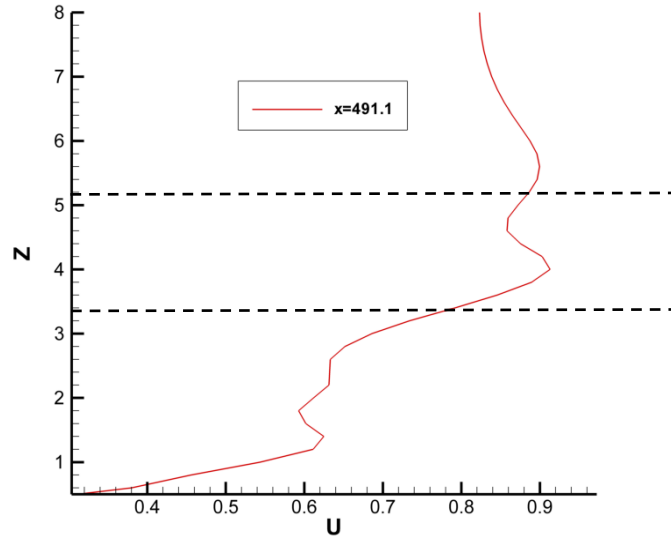


Figure 5: Streamwise Velocity Profile

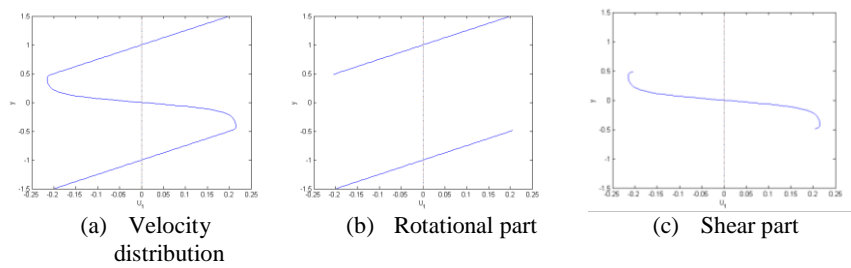


Figure 6: Case 1

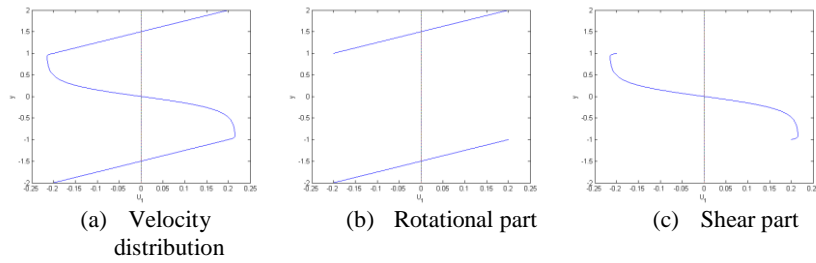


Figure 7: Case 2

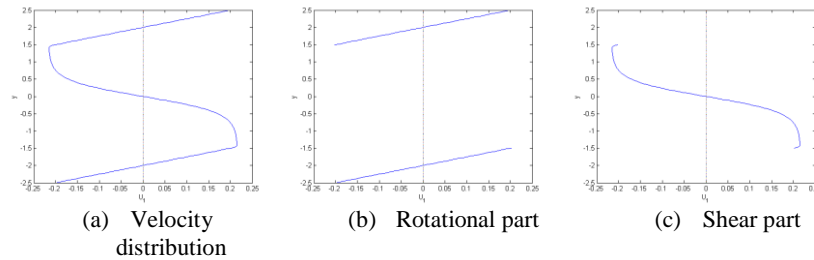


Figure 8: Case 3

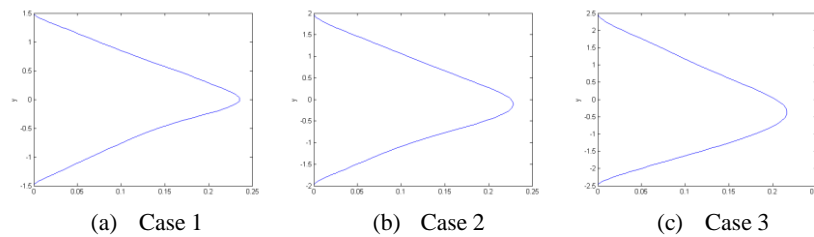


Figure 9: Corresponding profile of the eigenvector function for three cases

## References

- [1] Chen, L., Liu, X., Oliveira, M., Tang, D., Liu, C., Vortical Structure, Sweep and Ejection Events in Transitional Boundary Layer, Science China, Series G, Physics, Mechanics, Astronomy, Vol. 39 (10) pp1520-1526, 2009
- [2] Chen, L., Liu, X., Oliveira, M., Liu, C., DNS for ring-like vortices formation and roles in positive spikes formation, AIAA Paper 2010-1471, Orlando, FL, January 2010a.
- [3] Chen L., Tang, D., Lu, P., Liu, C., Evolution of the vortex structures and turbulent spots at the late-stage of transitional boundary layers, Science China, Physics, Mechanics and Astronomy, Vol. 53 No.1: 1–14, January 2010b,
- [4] Chen, L., Liu, C., Numerical Study on Mechanisms of Second Sweep and Positive Spikes in Transitional Flow on a Flat Plate, Journal of Computers and Fluids, Vol 40, pp28-41, 2011a
- [5] Chen, L., Liu, X., Tang, D., Liu, C. Evolution of the vortex structures and turbulent spots at the late-stage of transitional boundary layers. Science of China, Physics, Mechanics & Astronomy, 2011 Vol. 54 (5): 986-990, 2011b
- [6] Davidson, P. A., *Turbulence: An Introduction for Scientists and Engineers*. Oxford University Press. ISBN 9780198529491, 2004
- [7] F. Ducros, P. Comte and M. Lesieur. Large-eddy simulation of transition to turbulence in a boundary layer developing spatially over a flat plate. *J. Fluid Mech*, 326:1-36, 1996;

- [8] Jeong J., Hussain F. On the identification of a vortex, *J. Fluid Mech.* 1995, 285:69-94
- [9] Liu, C., and Liu, Z., Multigrid mapping and box relaxation for simulation of the whole process of flow transition in 3-D boundary layers, *J. of Computational Physics*, Vol. 119, pp. 325-341, 1995.
- [10] Liu, Z., Xiong, G., and Liu, C., Direct numerical simulation for the whole process of transition on 3-D airfoils. AIAA paper, AIAA 96-2081, 1996
- [11] Liu, C., and Liu, Direct Numerical Simulation for Flow Transition Around Airfoils, Proceedings of First AFOSR International Conference on DNS/LES, Louisiana Tech University, Ruston, Louisiana, August 4-8, 1997.
- [12] Liu, C., Chen, L., Study of mechanism of ring-like vortex formation in late flow transition, AIAA Paper 2010-1456, Orlando, FL, 2010a.
- [13] Liu, X., Chen, L., Oliveira, M., Tang, D., Liu, C., DNS for late stage structure of flow transition on a flat-plate boundary layer, AIAA Paper 2010-1470, Orlando, FL, January 2010b.
- [14] Liu, C., Chen, L., Study of mechanism of ring-like vortex formation in late flow transition, AIAA Paper 2010-1456, Orlando, FL, January 2010c.
- [15] Liu, X., Chen, Z., Liu, C., Late-Stage Vortical Structures and Eddy Motions in Transitional Boundary Layer Status, *Chinese Physics Letters* Vol. 27, No.2, pp.024706-1-4, 2010d
- [16] Liu, C., Chen, L., Lu, P., New Findings by High Order DNS for Late Flow Transition in a Boundary Layer, *J of Modeling and Simulation in Engineering*, Vol 2011, No.721487, pp.1-16, 2011a
- [17] Liu, C., Chen, L., Parallel DNS for vortex structure of late stages of flow transition, *J. of Computers and Fluids*, Vol.45, pp 129–137, 2011b
- [18] Liu, C., Numerical and Theoretical Study on “Vortex Breakdown”, *International Journal of Computer Mathematics*, Vol 88, Issue 17, , pp 3702-3708, 2011c
- [19] Liu, C., Chen, L., Lu, P., and Liu, X., Study on Multiple Ring-Like Vortex Formation and Small Vortex Generation in Late Flow Transition on a Flat Plate, *Theoretical and Numerical Fluid Dynamics*, Vol 27, Issue 1, pp.41-70, 2013
- [20] Lu, P., Liu, C., Numerical Study of Mechanism of U-Shaped Vortex Formation, AIAA Paper 2011-0286
- [21] Lu, P., Wang, Z., Chen, L. and Liu, C., Numerical study on U-shaped vortex formation in late boundary layer transition *Computers & Fluids* Vol. 55, pp.36-47, 2011a.
- [22] Lu, P. and Liu, C., Numerical study on mechanism of small vortex generation in boundary layer transition. AIAA Paper 2011-0287, 2011b

- [23] Lu, P. and Liu, C., DNS Study on Mechanism of Small Length Scale Generation in Late Boundary Layer Transition, *Physica D: Nonlinear Phenomena*, 241 (2012) 11-24, 2011c
- [24] Lu, P., Thampa, M, Liu, C., Numerical Study on Randomization in Late Boundary Layer Transition, AIAA 2012-0748, 2012
- [25] Marshak, Alex, *3D radiative transfer in cloudy atmospheres; pg.76*. Springer. ISBN 9783540239581, 2005
- [26] MEYER, D.G.W.; RIST, U.; KLOKER, M.J. (2003): Investigation of the flow randomization process in a transitional boundary layer. In: Krause, E.; Jäger, W. (eds.): *High Performance Computing in Science and Engineering '03*. Transactions of the HLRS 2003, pp. 239-253 (partially coloured), Springer.
- [27] Mullin, Tom, Turbulent times for fluids, *New Scientist.*, 11 November 1989
- [28] USA Today, Turbulence theory gets a bit choppy, September 10, 2006. [http://usatoday30.usatoday.com/tech/science/columnist/vergano/2006-09-10-turbulence\\_x.htm](http://usatoday30.usatoday.com/tech/science/columnist/vergano/2006-09-10-turbulence_x.htm)